THE JOURNAL OF PHYSICAL CHEMISTRY C
A JOURNAL OF THE AMERICAN CHEMICAL SOCIETY

pubs.acs.org/JPCC

Article

Relative Dye Adsorption Method for Determining the Hydrophobicity of Nanoparticles

Guangle Li, Kacie K. H. Y. Ho, and Yi Y. Zuo*

Cite This: *J. Phys. Chem. C* 2022, 126, 832−837

Read Online

ACCESS | Metrics & More | Article Recommendations | Supporting Information

ABSTRACT: The hydrophobicity of nanoparticles (NPs) is a crucial physicochemical property that determines the agglomeration state of NPs under various environmental and biological conditions. It plays a predominant role in determining the toxicity and environmental, health, and safety impact of NPs. However, to date, there is not yet a well-accepted standard method for characterizing the hydrophobicity of NPs. Here, we developed a relative dye adsorption method for determining the hydrophobicity of NPs. This method is modified from the traditional dye partitioning method that uses either the hydrophobic dye, rose bengal (RB), or the hydrophilic dye, Nile blue (NB). By studying the partitioning quotient for both RB and NB, the relative dye adsorption method eliminates the uncertainty introduced by estimating the surface area of NPs dispersed in liquid phases. We have demonstrated the applicability and accuracy of this method by comparing them to the hydrophobicity of NPs determined with the maximum particle dispersion method. It is concluded that the relative dye adsorption method can be used as a more reliable technique than RB or NB partitioning for determining the hydrophobicity of NPs.

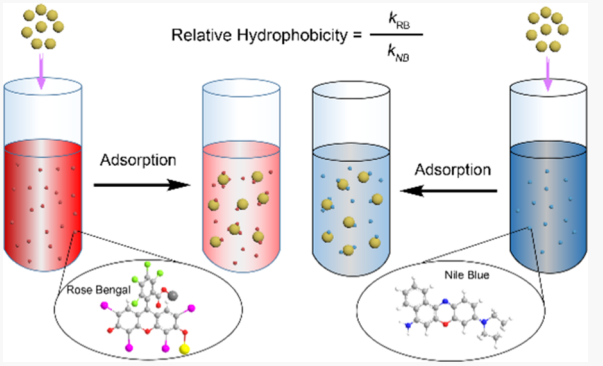

INTRODUCTION

Exposure of engineered nanoparticles (NPs) to the environment has rapidly increased due to their extensive scientific and industrial applications.[1] Understanding interactions between NPs and the environment as well as living organisms is of great importance for regulation and mitigation of the environmental, health, and safety (EHS) impact of NPs.[2] Effective characterization of physicochemical properties of NPs is a fundamental requirement for investigating their EHS impact and for ultimately assessing their environmental risk and toxicity. Consequently, significant efforts have been devoted to the development of standard characterization methods for determining various physicochemical properties of NPs, such as their size, shape, surface area, charge, chemical composition, and crystal structure.[3,4]

Among all physicochemical properties, the hydrophobicity of NPs plays a predominant role in determining the aggregation and deposition of NPs in various environmental conditions.[5,6] For example, it is found that the environmental fate and impact of microplastics and nanoplastics largely depend on the surface properties of these particles.[7,8] The hydrophobicity of colloidal plastic particles significantly influences their ability as a transport vector for environmental pollutants.[7,9] When interacting with biological systems, including NP entrance into the human body *via* respiratory, oral, or dermal portals, it has been found that the hydrophobicity of NPs regulates the formation of biomolecular corona, cellular uptake, phagocytic clearance, immune response, and translocation of NPs.[10−13] Hence, characterization of the hydrophobicity of NPs has become a necessity for assessing the EHS impact of NPs and for the safe design of inhaled nanomedicines.

Many methods have been developed for qualitatively and quantitatively determining the hydrophobicity of NPs, such as the contact angle method,[14,15] octanol−water partitioning,[5,16,17] inverse gas chromatography,[18] and maximum particle dispersion (MPD).[19] Among all available methods, rose bengal (RB) partitioning is a commonly used dye partitioning method.[20,21] RB is an anionic water-soluble xanthene dye that is widely used as a photosensitizer for many biomedical applications,[22,23] such as a stain of the ocular surface for diagnosis and treatment of dry eye disease.[24] RB is considered to be a hydrophobic dye as it selectively adsorbs to hydrophobic surfaces via its xanthene ring. Figure S1A, Supporting Information (SI), shows the chemical structure of the RB molecule. In general, RB partitioning measures the partitioning quotient (PQ) of the dye, i.e., the ratio of RB bound to the NP surface to free RB suspending in the liquid

Received: November 6, 2021
Revised: December 15, 2021
Published: December 29, 2021

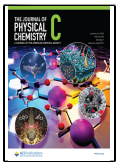

phase. The relative hydrophobicity of a series of NPs can be compared by plotting their PQs against the surface areas of the NPs, where a larger slope of the linear regression of the plot indicates more hydrophobic NPs.[20,21]

The RB partitioning method has demonstrated its usefulness in qualitatively characterizing the hydrophobicity of NPs for studying their toxicity and EHS impact.[5,13,25,26] Nevertheless, this method has two major limitations. First, due to the hydrophobic nature of the dye, RB partitioning only provides robust measurements for relatively hydrophobic NPs.[5] Second, its accuracy heavily depends on the estimation of NPs' surface area, which is not a trivial task due to the highly dynamic and heterogeneous process of particle aggregation and agglomeration in the liquid phase. A large heterogeneity of particles aggregation is not unexpected for incidental particles, such as microplastics and nanoplastics,[7,8] which would further complicate the determination of a representative surface area needed in the traditional dye partitioning methods. In the classical RB partitioning method, the total surface area of the NPs dispersed in the suspension was estimated from their hydrodynamic sizes by assuming a spherical shape, which further introduces errors to heterogeneous and/or nonspherical NPs.

To overcome the first limitation, Xiao and Wiesner have introduced a hydrophilic dye, Nile blue (NB), which can be used as a counterpart of RB for determining the hydrophobicity of relatively hydrophilic NPs, such as fullerol and noble metal NPs.[5] NB is a cationic benzophenoxazine dye. It has been used in photodynamic therapy owing to its affinity to lipid membranes and localization in lysosomes, which can be subsequently uptaken by tumor cells.[27] NB has a hydrophilic amino group and a positively charged planar aromatic moiety, which makes it preferably affiliated to hydrophilic surfaces. Figure S1B shows the chemical structure of NB. Compared to RB, NB partitioning results in a larger PQ slope for less hydrophobic NPs, thus circumventing the limitation of RB partitioning in studying hydrophilic NPs. However, NB partitioning suffers from the same limitation of RB partitioning in terms of accurately determining the surface area of NPs dispersed in liquids.

Here, we developed a relative dye adsorption method for determining the hydrophobicity of NPs. By studying PQs for both RB and NB, the relative dye adsorption method eliminates the uncertainty introduced by estimating the surface area of dispersed NPs. We have demonstrated the applicability and accuracy of this method, by comparing the obtained NP hydrophobicity values with values determined using the maximum particle dispersion method.[19] We concluded that the relative dye adsorption method can be used as a more reliable technique than RB or NB partitioning for determining the hydrophobicity of NPs.

EXPERIMENTAL SECTION

Materials. Nanoparticles (NPs) were obtained from commercial sources summarized in Table 1. Rose bengal (RB) and Nile blue A (NB) were purchased from Sigma-Aldrich. Phosphate-buffered saline (PBS, 10× solution) was purchased from Fisher Scientific. Water used was Milli-Q ultrapure water (Millipore) with a resistivity greater than 18 MΩ·cm at room temperature. The morphologies of NPs were characterized by scanning electron microscopy (Hitachi S-4800). The primary size of NPs was analyzed from the electron micrographs using ImageJ. The hydrodynamic size and ζ-

Table 1. Summary of the Nanoparticles (NPs) Studied

NPs	source	primary size (nm)	hydrodynamic size (nm)[a]	PDI[a]	ζ-potential (mV)[a]	hydrophobicity determined by RB partitioning (10^{-9} mL/μm^2)	hydrophilicity determined by NB partitioning (10^{-9} mL/μm^2)	RB/NB dye adsorption ratio	SFE by MPD (mJ/m^2)
TCS-ZnO	JRC, European Commission	59 ± 19 (diameter) 144 ± 42 (length)	467 ± 15	0.372 ± 0.064	−33.4 ± 3.8	0.265 ± 0.004	0.652 ± 0.022	0.406 ± 0.019	21.2 ± 0.4
ZnO	JRC, European Commission	55 ± 16 (diameter) 159 ± 35 (length)	470 ± 46	0.463 ± 0.116	−47.7 ± 3.9	0.007 ± 0.0008	0.025 ± 0.004	0.282 ± 0.075	29.3 ± 0.5
BN	Sigma-Aldrich	122 ± 39	475 ± 13	0.291 ± 0.067	−48.3 ± 3.6	0.162 ± 0.012	0.840 ± 0.088	0.193 ± 0.035	32.9 ± 0.1
PST	Thermo Scientific	707 ± 12	796 ± 41	0.137 ± 0.065	−77.2 ± 6.6	0.016 ± 0.004	0.851 ± 0.081	0.018 ± 0.006	36.4 ± 1.4

[a]TCS-ZnO, triethoxycaprylysilane-coated zinc oxide; ZnO, zinc oxide; BN, boron nitride; PST, polystyrene; JRC, joint research center repository of representative industrial nanomaterials; PDI, polydispersity index; SFE, surface free energy; and MPD, maximum particle dispersion method. The hydrodynamic size, PDI, and ζ-potential of these NPs were measured in the PBS solution (pH 7.4).

https://doi.org/10.1021/acs.jpcc.1c09610
J. Phys. Chem. C 2022, 126, 832−837

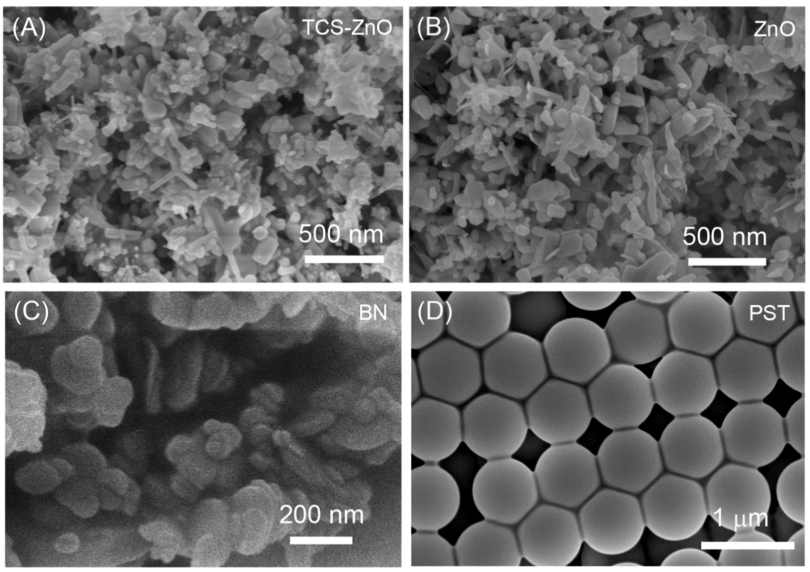

Figure 1. Scanning electron microscopy (SEM) micrographs showing the morphology of the studied nanoparticles (NPs). (A) Triethoxycaprylysilane-coated zinc oxide (TCS-ZnO), (B) zinc oxide (ZnO), (C) boron nitride (BN), and (D) polystyrene (PST).

potential of NPs were determined using Zetasizer Nano ZS (Malvern Panalytical).

Relative Dye Adsorption Method. The relative dye adsorption method requires separately determining the partitioning quotient (PQ) of both the hydrophobic dye, RB, and the hydrophilic dye, NB. About 2 mg/mL dye (RB or NB) solution was diluted to 20 μg/mL using the PBS solution. Stock solutions for NPs were prepared at the following concentrations: triethoxycaprylysilane-coated zinc oxide (TCS-ZnO), zinc oxide (ZnO), and boron nitride (BN) NPs each at 5 mg/mL, and polystyrene (PST) NPs at 10 mg/mL. A series of NP stock solutions were added to the dye solution to create a wide array of dye−NP suspensions. Controls were prepared by adding the same volume of dispersion liquid to the dye solution to account for the slight increasing volume due to the added NP stock solution. All suspensions were incubated at room temperature for 3 h and subsequently centrifuged at 16 000g for 1 h. Supernatants were collected, and dye molecules in supernatants were analyzed with a UV−vis spectrometer (Epoch, BioTek) at 549 nm for RB and 620 nm for NB, respectively. The PQ was calculated by the ratio of the dye bound onto the NP surface (D_{bound}) to free dye molecules in the liquid phase (D_{free}), i.e., PQ = D_{bound}/D_{free}. PQ vs the surface area of NPs was plotted, and the slope of the linear regression line was obtained using OriginPro. The total surface area of NPs dispersed in the suspension was calculated from the hydrodynamic size of these NPs determined with dynamic light scattering, by assuming a spherical shape. The relative dye adsorption was calculated by taking the ratio between the slopes for the linear regression of RB and NB. As demonstrated in eqs S1−S7 in the SI, the use of relative dye adsorption eliminates uncertainties in determining the surface areas of the dispersed NPs.

Maximum Particle Dispersion Method. The maximum particle dispersion (MPD) method was implemented as previously described.[19] The MPD is an optical method for quantitatively determining the surface free energy of NPs. It relies on a novel measuring principle of quantitatively evaluating the colloidal stability of NP suspensions determined by the balance between van der Waals attraction and electrostatic repulsion. In brief, a trace amount of the NP stock solution was added to a series of probing liquids of 0.5 mL each. The probing liquids consist of a nonpolar liquid set, including six alkanes ranging from C_5 to C_{16} and covering the surface tension range of 16−27 mJ/m^2, and a polar liquid set made of water/ethanol mixtures, covering the surface tension range of 22.3−71.4 mJ/m^2. After vortexed, the mixtures were centrifuged at 100g for 5 min for ZnO and BN NPs, and at 800g for 10 min for PST NPs to allow particle sedimentation. Subsequently, 160 μL of the supernatant from each suspension was transferred to a 96-well microplate without disturbing the sediment. The optical density at 400 nm (OD_{400}) was measured using a microplate reader (Epoch, BioTek). The optical density was plotted against the surface tensions of the probing liquids, and the surface free energy of NPs was determined at the maximum optical density value obtained by optimal peak fitting using OriginPro. Each measurement was repeated at least three times, and the results were shown as mean ± standard deviation.

RESULTS AND DISCUSSION

Figure 1 shows the electron micrographs of four nanoparticles (NPs), i.e., triethoxycaprylysilane-coated zinc oxide (TCS-ZnO), zinc oxide (ZnO), boron nitride (BN), and polystyrene (PST) NPs. As shown in Table 1, TCS-ZnO, ZnO, and BN NPs have similar hydrodynamic sizes of 467, 470, and 475 nm, respectively. These are much larger than their corresponding primary sizes. PST NPs, on the other hand, have a hydrodynamic size of 796 nm, which is close to their primary size of 707 nm. Figure S2 shows the size distributions of these four NPs in PBS. Except for PST NPs, which demonstrate a narrower size distribution, the other three NPs display a bimodal distribution with a majority of particles distributed in the size range between 100 and 1000 nm, and hence they show a larger polydispersity index (PDI) than PST NPs.

The ζ-potentials of TCS-ZnO, ZnO, and BN NPs in PBS are −33.4, −47.7, and −48.3 mV, respectively, while PST NPs have a significantly more negative ζ-potential of −77.2 mV, thus indicating more electrostatic repulsion between PST NPs

https://doi.org/10.1021/acs.jpcc.1c09610
J. Phys. Chem. C 2022, 126, 832−837

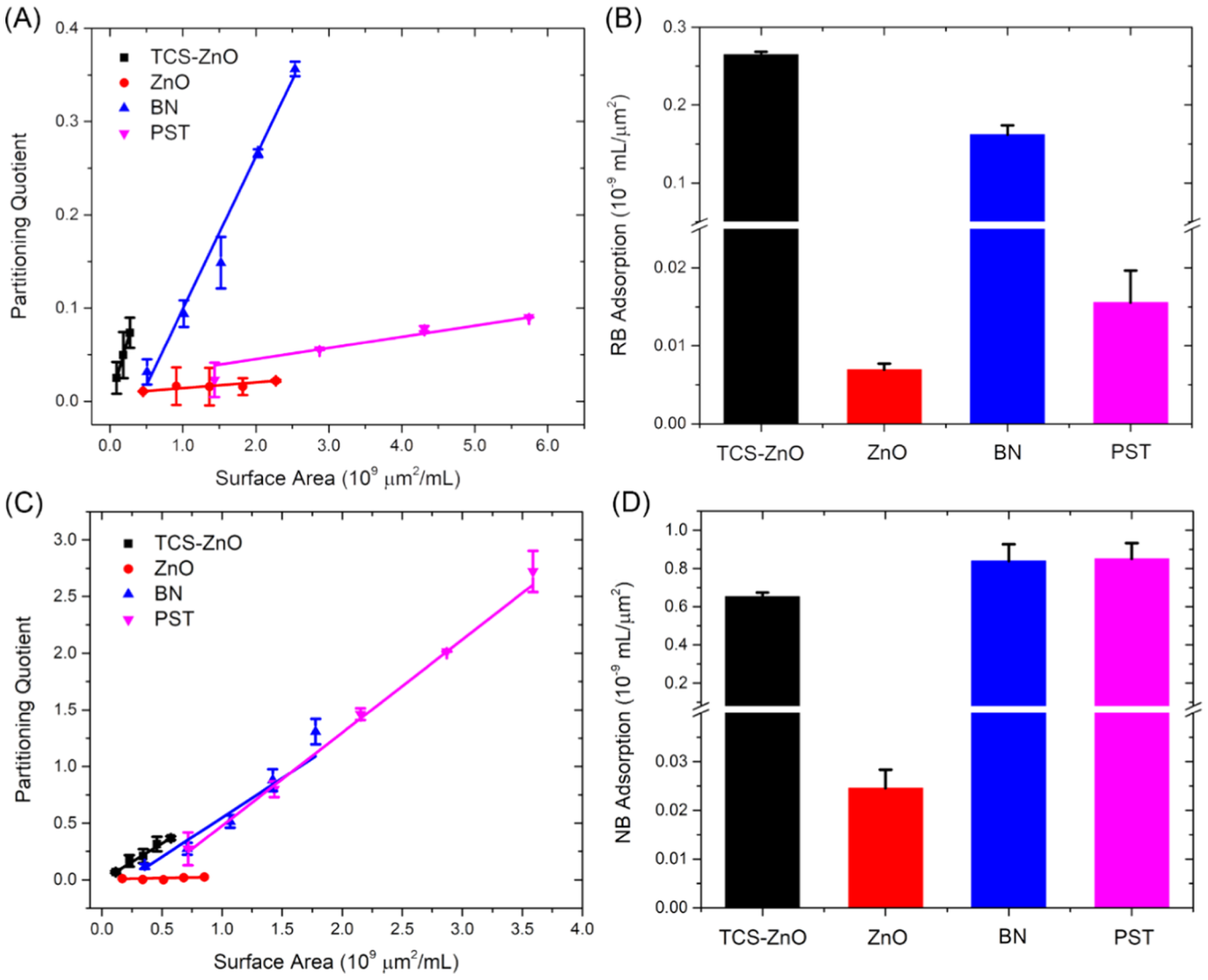

Figure 2. Determination of the hydrophobicity/hydrophilicity of four NPs, i.e., TCS-ZnO, ZnO, BN, and PST NPs. (A) Linear regression of the partitioning quotient (PQ) of rose bengal (RB) against the surface areas of NPs. (B) RB adsorption, corresponding to the rank of NP hydrophobicity, determined with the RB partitioning method. (C) Linear regression of the PQ of Nile blue (NB) against the surface areas of NPs. (D) NB adsorption, corresponding to the rank of NP hydrophilicity, determined with the NB partitioning method.

than the other NPs. This ζ-potential measurement is consistent with the lack of aggregation found for PST NPs.

Figure 2A shows the hydrophobicity measurement with the RB partitioning method, in which the slope of the plot, i.e., RB adsorption, is proportional to the hydrophobicity of NPs. As shown in Figure 2B, the hydrophobicity of these NPs is ranked as TCS-ZnO > BN > PST > ZnO. Figure 2C shows the dye partitioning method with NB, in which the slope of the plot, i.e., NB adsorption, is proportional to the hydrophilicity of NPs. As shown in Figure 2D, the hydrophilicity of these NPs is ranked as PST ≈ BN > TCS-ZnO > ZnO. Comparing results obtained with both RB and NB partitioning, an obvious discrepancy occurs to ZnO NPs. While RB partitioning predicts that ZnO is the least hydrophobic out of the four NPs studied, NB partitioning predicts that ZnO is the least hydrophilic (i.e., the most hydrophobic) among the four NPs tested.

In general, it is found that the adsorption capacity of NB for all tested NPs is significantly higher than that of RB (Figure 2B vs 2D). It should be noted that the adsorption of dyes onto NP surfaces is not only affected by hydrophobic interactions but also by electrostatic interactions. The isoelectric points for TCS-ZnO, ZnO, BN, and PST NPs are reported to be around 2.7, 3.9, 4.3, and 3.8, respectively.[28−30] Consequently, all of these NPs are negatively charged at pH 7.4 (Table 1), thus attracting more the cationic dye NB than the anionic dye RB. Hence, it is not meaningful to directly compare the adsorption capacity of RB and NB onto NPs. In addition, the adsorption kinetics is highly sensitive to the surface area of NPs, which cannot be measured in situ. It is found that the PQ slope is highly dependent on the estimation of NPs' surface area. In the traditional dye (RB or NB) partitioning method, the hydrodynamic size of NPs is used to calculate their surface area by assuming a spherical shape of NP aggregates in the dye solution. When the NPs' surface area is calculated with other means, e.g., using the primary size of NPs (Figures S3 and S4), the hydrophobicity results determined with either RB or NB portioning were found to be varying.

Figure 3 shows the results of the relative dye adsorption method. By taking the ratio between the RB adsorption and

https://doi.org/10.1021/acs.jpcc.1c09610
J. Phys. Chem. C 2022, 126, 832−837

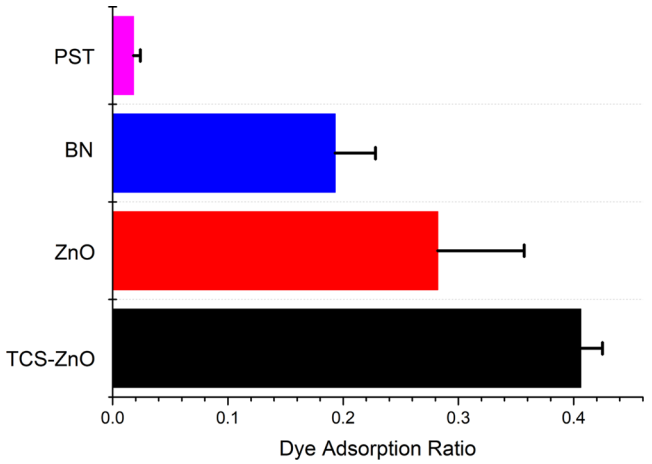

Figure 3. Hydrophobicity of four NPs, i.e., TCS-ZnO, ZnO, BN, and PST NPs, determined with the relative dye adsorption method. The RB/NB dye adsorption ratio is defined as the ratio between the hydrophobic dye, RB (Figure 2B), and the hydrophilic dye, NB (Figure 2D). Results suggest that the hydrophobicity of these NPs ranks as TCS-ZnO > ZnO > BN > PST.

the NB adsorption, the dye adsorption ratio is proportional to the hydrophobicity of NPs while eliminating uncertainties introduced from the estimation of NP's surface area. Based on dye adsorption ratio values, the hydrophobicity of NPs can be ranked in the order of TCS-ZnO > ZnO > BN > PST. To verify this result, we have measured the surface free energy (SFE) of these NPs using the independent maximum particle dispersion method (Figure S5).[19] The SFEs of TCS-ZnO, ZnO, BN, and PST NPs are determined at 21.2, 29.3, 32.9, and 36.4 mJ/m^2, respectively (Table 1), which correspond to a hydrophobicity rank of TCS-ZnO > ZnO > BN > PST, in good agreement with the rank determined with the relative dye adsorption method.

It should be noted that Crandon *et al.* also used these two dyes to determine the hydrophobicity of NPs.[31] In their method, adsorption isotherms were obtained by varying the dye concentration at a constant NP concentration. The adsorption isotherms were fit to linear, Langmuir, and Freundlich models, and a dimensionless parameter termed hydrophobicity ratio was defined by the ratio of adsorption constant of RB and NB obtained from the linear fitting model. This procedure also eliminates the necessity for the calculation of the surface area of NPs. However, the slope of the linear fitting curve represents the adsorption kinetics, instead of the relative hydrophobicity or hydrophilicity of NPs. In addition, varying the dye concentration may introduce uncertainties as the absorption peak of the dye depends on its concentration. It was reported that the adsorption peak of NB derivatives shifts to blue with increasing concentrations from 4.0 to 32.0 μM.[32] In contrast, the dye concentration used in our method is fixed.

CONCLUSIONS

We have developed a relative dye adsorption method for determining the hydrophobicity of NPs. This method is modified from the traditional dye partitioning method that uses either the hydrophobic dye, rose bengal (RB), or the hydrophilic dye, Nile blue (NB). By studying the partitioning quotient for both RB and NB, the relative dye adsorption method eliminates the uncertainty introduced by estimating the surface area of NPs dispersed in liquid phases. We have demonstrated the applicability and accuracy of the method by comparing it to the hydrophobicity of NPs determined with the maximum particle dispersion method. It is concluded that the relative dye adsorption method can be used as a more reliable technique than RB or NB partitioning for determining the hydrophobicity of NPs.

ASSOCIATED CONTENT

Supporting Information

The Supporting Information is available free of charge at https://pubs.acs.org/doi/10.1021/acs.jpcc.1c09610.

Chemical structures of rose bengal and Nile blue (Figure S1); size distribution of NPs in PBS (Figure S2); uncertainties of RB and NB partitioning methods when using the primary particle size to estimate the surface area of NPs (Figures S3 and S4); surface free energy of NPs determined with the maximum particle dispersion method (Figure S5); and calculation of the dye adsorption ratio (eqs S1−S7) (PDF)

AUTHOR INFORMATION

Corresponding Author

Yi Y. Zuo − *Department of Mechanical Engineering, University of Hawaii at Manoa, Honolulu, Hawaii 96822, United States; Department of Pediatrics, John A. Burns School of Medicine, University of Hawaii, Honolulu, Hawaii 96826, United States;* orcid.org/0000-0002-3992-3238; Phone: 808-956-9650; Email: yzuo@hawaii.edu; Fax: 808-956-2373

Authors

Guangle Li − *Department of Mechanical Engineering, University of Hawaii at Manoa, Honolulu, Hawaii 96822, United States*

Kacie K. H. Y. Ho − *Department of Human Nutrition, Food and Animal Sciences, University of Hawaii at Manoa, Honolulu, Hawaii 96822, United States*

Complete contact information is available at: https://pubs.acs.org/10.1021/acs.jpcc.1c09610

Author Contributions

Y.Y.Z. designed the research; G.L. performed the experiments and analyzed the data; K.K.H.Y.H. analyzed the dynamic light scattering data; and G.L. and Y.Y.Z. drafted the paper. All authors approved the final version of the manuscript.

Notes

The authors declare no competing financial interest.

ACKNOWLEDGMENTS

This research was supported by the National Science Foundation Grant no. CBET-2011317 (Y.Y.Z.).

REFERENCES

(1) Mueller, N. C.; Nowack, B. Exposure Modeling of Engineered Nanoparticles in the Environment. *Environ. Sci. Technol.* **2008**, *42*, 4447−4453.

(2) Nel, A. E.; Mädler, L.; Velegol, D.; Xia, T.; Hoek, E. M. V.; Somasundaran, P.; Klaessig, F.; Castranova, V.; Thompson, M. Understanding biophysicochemical interactions at the nano−bio interface. *Nat. Mater.* **2009**, *8*, 543−557.

(3) Nel, A.; Xia, T.; Madler, L.; Li, N. Toxic potential of materials at the nanolevel. *Science* **2006**, *311*, 622−627.

(4) Hussain, S. M.; Braydich-Stolle, L. K.; Schrand, A. M.; Murdock, R. C.; Yu, K. O.; Mattie, D. M.; Schlager, J. J.; Terrones, M. Toxicity Evaluation for Safe Use of Nanomaterials: Recent Achievements and Technical Challenges. *Adv. Mater.* **2009**, *21*, 1549−1559.
(5) Xiao, Y.; Wiesner, M. R. Characterization of surface hydrophobicity of engineered nanoparticles. *J. Hazard. Mater.* **2012**, *215*−*216*, 146−151.
(6) Petosa, A. R.; Jaisi, D. P.; Quevedo, I. R.; Elimelech, M.; Tufenkji, N. Aggregation and deposition of engineered nanomaterials in aquatic environments: role of physicochemical interactions. *Environ. Sci. Technol.* **2010**, *44*, 6532−6549.
(7) Alimi, O. S.; Farner Budarz, J.; Hernandez, L. M.; Tufenkji, N. Microplastics and Nanoplastics in Aquatic Environments: Aggregation, Deposition, and Enhanced Contaminant Transport. *Environ. Sci. Technol.* **2018**, *52*, 1704−1724.
(8) Gigault, J.; El Hadri, H.; Nguyen, B.; Grassl, B.; Rowenczyk, L.; Tufenkji, N.; Feng, S.; Wiesner, M. Nanoplastics are neither microplastics nor engineered nanoparticles. *Nat. Nanotechnol.* **2021**, *16*, 501−507.
(9) Teuten, E. L.; Rowland, S. J.; Galloway, T. S.; Thompson, R. C. Potential for plastics to transport hydrophobic contaminants. *Environ. Sci. Technol.* **2007**, *41*, 7759−7764.
(10) Oberdörster, G.; Oberdörster, E.; Oberdörster, J. Nanotoxicology: an emerging discipline evolving from studies of ultrafine particles. *Environ. Health Perspect.* **2005**, *113*, 823−839.
(11) Verma, A.; Stellacci, F. Effect of Surface Properties on Nanoparticle−Cell Interactions. *Small* **2010**, *6*, 12−21.
(12) Moyano, D. F.; Goldsmith, M.; Solfiell, D. J.; Landesman-Milo, D.; Miranda, O. R.; Peer, D.; Rotello, V. M. Nanoparticle Hydrophobicity Dictates Immune Response. *J. Am. Chem. Soc.* **2012**, *134*, 3965−3967.
(13) Valle, R. P.; Huang, C. L.; Loo, J. S. C.; Zuo, Y. Y. Increasing Hydrophobicity of Nanoparticles Intensifies Lung Surfactant Film Inhibition and Particle Retention. *ACS Sustainable Chem. Eng.* **2014**, *2*, 1574−1580.
(14) Wang, S.; Zhang, Y.; Abidi, N.; Cabrales, L. Wettability and Surface Free Energy of Graphene Films. *Langmuir* **2009**, *25*, 11078−11081.
(15) Azimi, G.; Dhiman, R.; Kwon, H.-M.; Paxson, A. T.; Varanasi, K. K. Hydrophobicity of rare-earth oxide ceramics. *Nat. Mater.* **2013**, *12*, 315−320.
(16) Jafvert, C. T.; Kulkarni, P. P. Buckminsterfullerene's (C60) Octanol−Water Partition Coefficient (Kow) and Aqueous Solubility. *Environ. Sci. Technol.* **2008**, *42*, 5945−5950.
(17) Praetorius, A.; Tufenkji, N.; Goss, K.-U.; Scheringer, M.; von der Kammer, F.; Elimelech, M. The road to nowhere: equilibrium partition coefficients for nanoparticles. *Environ. Sci.: Nano* **2014**, *1*, 317−323.
(18) Das, S. C.; Larson, I.; Morton, D. A. V.; Stewart, P. J. Determination of the Polar and Total Surface Energy Distributions of Particulates by Inverse Gas Chromatography. *Langmuir* **2011**, *27*, 521−523.
(19) Cao, Z.; Tsai, S. N.; Zuo, Y. Y. An Optical Method for Quantitatively Determining the Surface Free Energy of Micro- and Nanoparticles. *Anal. Chem.* **2019**, *91*, 12819−12826.
(20) Müller, R. H.; Rühl, D.; Lück, M.; Paulke, B. R. Influence of Fluorescent Labelling of Polystyrene Particles on Phagocytic Uptake, Surface Hydrophobicity, and Plasma Protein Adsorption. *Pharm. Res.* **1997**, *14*, 18−24.
(21) Doktorovova, S.; Shegokar, R.; Martins-Lopes, P.; Silva, A. M.; Lopes, C. M.; Müller, R. H.; Souto, E. B. Modified Rose Bengal assay for surface hydrophobicity evaluation of cationic solid lipid nanoparticles (cSLN). *Eur. J. Pharm. Sci.* **2012**, *45*, 606−612.
(22) Vanerio, N.; Stijnen, M.; de Mol, B. A. J. M.; Kock, L. M. Biomedical Applications of Photo- and Sono-Activated Rose Bengal: A Review. *Photobiomodulation, Photomed., Laser Surg.* **2019**, *37*, 383−394.
(23) Gianotti, E.; Martins Estevão, B.; Cucinotta, F.; Hioka, N.; Rizzi, M.; Renò, F.; Marchese, L. An Efficient Rose Bengal Based Nanoplatform for Photodynamic Therapy. *Chem. - Eur. J.* **2014**, *20*, 10921−10925.
(24) Doughty, M. J. Rose bengal staining as an assessment of ocular surface damage and recovery in dry e ye disease—A review. *Contact Lens Anterior Eye* **2013**, *36*, 272−280.
(25) Yang, Y.; Xu, L.; Dekkers, S.; Zhang, L. G.; Cassee, F. R.; Zuo, Y. Y. Aggregation State of Metal-Based Nanomaterials at the Pulmonary Surfactant Film Determines Biophysical Inhibition. *Environ. Sci. Technol.* **2018**, *52*, 8920−8929.
(26) Beck-Broichsitter, M.; Ruppert, C.; Schmehl, T.; Guenther, A.; Betz, T.; Bakowsky, U.; Seeger, W.; Kissel, T.; Gessler, T. Biophysical investigation of pulmonary surfactant surface properties upon contact with polymeric nanoparticles in vitro. *Nanomed.: Nanotechnol. Biol. Med.* **2011**, *7*, 341−350.
(27) Martinez, V.; Henary, M. Nile Red and Nile Blue: Applications and Syntheses of Structural Analogues. *Chem. - Eur. J.* **2016**, *22*, 13764−13782.
(28) Dossier on Zinc Oxide Part 1. ENV/JM/MONO(2015)15/PART1.
(29) Wattanakul, K.; Manuspiya, H.; Yanumet, N. The adsorption of cationic surfactants on BN surface: Its effects on the thermal conductivity and mechanical properties of BN-epoxy composite. *Colloids Surf., A* **2010**, *369*, 203−210.
(30) Bolt, P. S.; Goodwin, J. W.; Ottewill, R. H. Studies on the Preparation and Characterization of Monodisperse Polystyrene Latices. VI. Preparation of Zwitterionic Latices. *Langmuir* **2005**, *21*, 9911−9916.
(31) Crandon, L. E.; Boenisch, K. M.; Harper, B. J.; Harper, S. L. Adaptive methodology to determine hydrophobicity of nanomaterials in situ. *PLoS One* **2020**, *15*, No. e0233844.
(32) Jose, J.; Ueno, Y.; Burgess, K. Water-Soluble Nile Blue Derivatives: Syntheses and Photophysical Properties. *Chem. - Eur. J.* **2009**, *15*, 418−423.

https://doi.org/10.1021/acs.jpcc.1c09610
J. Phys. Chem. C 2022, 126, 832−837